

See discussions, stats, and author profiles for this publication at: <https://www.researchgate.net/publication/233899591>

Amplifying Emission Enhancement and Proton Response in Two Component Gel.

ARTICLE *in* LANGMUIR · DECEMBER 2012

Impact Factor: 4.46 · DOI: 10.1021/la3037617 · Source: PubMed

CITATIONS

21

READS

35

8 AUTHORS, INCLUDING:



Pengchong Xue

Jilin University

79 PUBLICATIONS 1,588 CITATIONS

[SEE PROFILE](#)



Tierui Zhang

Technical Institute of Physics and Chemistry

110 PUBLICATIONS 3,276 CITATIONS

[SEE PROFILE](#)



Hirotaka Ihara

Kumamoto University

313 PUBLICATIONS 3,956 CITATIONS

[SEE PROFILE](#)

Amplifying Emission Enhancement and Proton Response in a Two-Component Gel

Pengchong Xue,*[†] Ran Lu,*[†] Peng Zhang,[†] Junhui Jia,[†] Qiuxia Xu,[†] Tierui Zhang,[‡] Makoto Takafuji,[§] and Hirotaka Ihara[§]

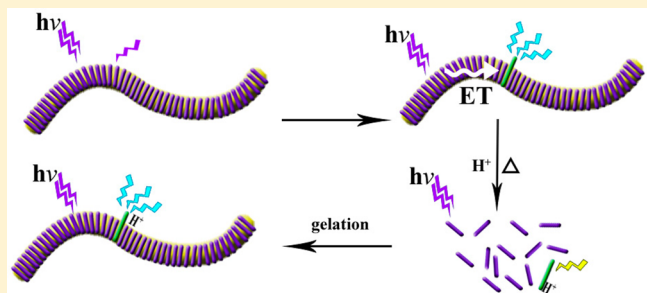
[†]State Key Laboratory of Supramolecular Structure and Materials, College of Chemistry, Jilin University, 2699# Changchun, 130061, China

[‡]Key Laboratory of Photochemical Conversion and Optoelectronic Materials, Technical Institute of Physics and Chemistry, Chinese Academy of Sciences, Beijing 100190, China

[§]Department of Applied Chemistry and Biochemistry, Kumamoto University, 2-39-1 Kurokami, Kumamoto, Japan

S Supporting Information

ABSTRACT: A glutamide gelator, **1**, was synthesized, and a weak emission enhancement was observed during its gelation. In addition, **1** could be an excellent scaffold for successfully embedding an energy acceptor, **2**, into its aggregate to obtain highly efficient energy transfer. An amplification of the emission enhancement was observed in the two-component gels compared to that of the neat gel of **1** during gel formation. For example, **1** induced only a 2.5-fold increase in emission intensity, whereas a 23-fold enhanced emission could be observed in the two-component gel with only 1.6 mol % **2**. Furthermore, two-component gels had an excited proton response. In systems with low acceptor concentrations, the hot solution red-shifted the fluorescence from blue to yellow upon the addition of a proton, which continuously blue-shifted with decreasing temperature to form the gel given that the binding of the gelator to the proton is weakened during coassembly. Moreover, the casting film formed by the two-component wet gel had an excellent response to volatile acids such as hydrochloric acid, trifluoroacetic acid, and so on and could be reversibly recovered by exposure to NH₃.



increased photocurrent.⁴ Furthermore, several two-component gels with energy-transfer properties have been developed to achieve tunable or white light emission.⁵ However, no example exists with respect to the study of the amplification of emission enhancement and the response to an external stimulus in two-component gels with energy-transfer properties.

In this article, we synthesized **1** and found that it presented weak fluorescence and a small enhanced emission (a 2.5-fold increase) during gelation because of the low fluorescence quantum yield (Φ_F) and H-aggregation formation. Therefore, another molecule, **2**, that has a high Φ_F was chosen to construct two-component gels with **1** as the energy donor (Scheme 1) because of its similar molecular structure to **1**. The results show that a small amount of **2** could completely quench the fluorescence of **1** because of the energy transfer from **1** to **2**. Such a two-component gel exhibited an amplification of emission enhancement compared to that of a neat gel of **1**. For example, the DMSO/H₂O solution of **1** (1.25 mM) with 1.6 mol % **2** increased its fluorescence intensity by 23-fold after

INTRODUCTION

Noncovalent interactions have received increasing attention as effective tools for the self-assembly of molecules with well-defined supramolecular structures that determine the properties of materials.¹ Increased interest in these interactions has occurred with respect to developing novel gel-phase materials based on small-molecular-mass gelators.² Their self-assembled process leads to the formation of supramolecular polymer-like structures that are driven by intermolecular noncovalent interactions. These suprastructures are useful in light-harvesting systems, photoswitches, sensors, drug delivery and release, medical therapy, ion recognition, templated transcription, solar cells, and so on.³

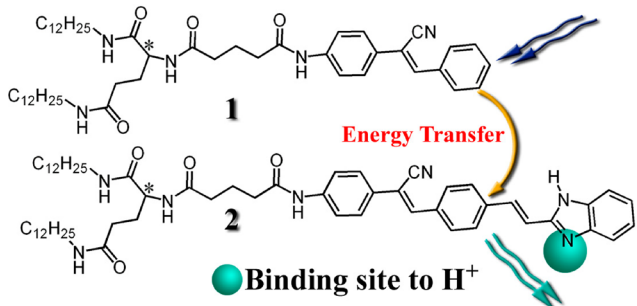
Organogels are jellylike soft materials that are generally composed of a one-component gelator and a significant amount of solvent. However, obtaining gels with special functions is sometimes difficult when only one gelator is used. A two-component gel can be used by introducing another active unit to overcome such a weakness. For example, several electron acceptors (iodine, 2,4,7-trinitrofluorenone, and fullerene derivatives) were introduced into the gels. In addition, charge-transfer and photoinduced electron-transfer complexes are formed to obtain high stability, high conductivity, and

Received: September 19, 2012

Revised: December 6, 2012

Published: December 11, 2012

Scheme 1. Molecular Structures of 1 and 2, the Energy Transfer Representation between Them, and the Proton-Binding Site Marking of 2



it was transferred to the gel phase. Moreover, the fluorescence emission of the two-component gels could be tuned by the ratio of the donor and the acceptor. After this, we studied the proton response of the two-component gels considering that the fluorescence of 2 is sensitive to protons.⁶ As a result, the two-component wet gels could function as fluorescent sensory materials for the proton. Moreover, drop-casted xerogel films of such two-component wet gels also exhibited a good reversible response to volatile acids such as hydrochloric acid, trifluoroacetic acid (TFA), and so on. As far as we know, this study is the first to regulate the properties of enhanced emission through another participant in the gel and the response of energy-transfer of the two-component gel to an external stimulus. This work may also lead to the development of two-component gels with superior properties.

EXPERIMENTAL SECTION

General Information. All raw materials were used without further purification. All solvents were purchased as analytical reagents from Beijing Chemical Works (Beijing, China) and were used without further purification. Water used throughout all experiments was purified with the Millipore system. Infrared spectra were measured using a Nicolet-360 Fourier transform infrared (FT-IR) spectrometer by incorporating the samples into KBr disks. The UV-vis absorption spectra were obtained using a Mapada UV-1800pc spectrophotometer. C, H, and N elemental analyses were performed on a Perkin-Elmer 240C elemental analyzer. Photoluminescence measurements were taken on a Shimadzu RF-5301 luminescence spectrometer. ¹H NMR spectra were carried out on Mercury plus 500 MHz spectrometer. Scanning electron microscope (SEM) images were carried out on a Japan Hitachi model X-650 scanning electron microscope. Fluorescence microscopy images were taken using an epifluorescence microscope (Olympus Reflected Fluorescence System BX51, Olym-

pus, Japan). Optical microscopy images were obtained using an XP-201 polarizing microscope. The specimens for SEM, fluorescence, and optical microscopy were prepared by a film-casting method. First, a small amount of wet gel was transferred to a glass slide, and then solvent was removed in a vacuum oven to obtain a xerogel film. Specimens for SEM observation were further coated with a thin layer of gold. The fluorescence quantum yields of 1 and 2 in DMSO were measured by comparing to a standard (quinine sulfate in 0.1 M H₂SO₄ solution). The excitation wavelength was 360 nm. Fluorescence lifetimes were measured using an FLS920 time-correlated single-photon counting (TCSPC) system. The excitation wavelength was 360 nm. The optical path length of the cells for absorption and fluorescence spectra was 1 mm.

Gelation Test of 1. The solution containing weighed gelator 1 in an organic solvent was heated in a sealed test tube with a diameter of 1 cm in an oil bath until the solid was dissolved. The solution was allowed to stand at room temperature for 6 h, and then the state of the mixture was evaluated by the stable to inversion of a test tube method.

Synthesis, Procedures, and Characterization. Compounds 2 and 3 were synthesized by the procedure reported previously.⁷

N1-((1,3-Bis(dodecylcarbamoyl)propylcarbamoyl)-N5-(4-(1-cyano-2-phenylvinyl)phenyl) Glutaramide (1). Compound 3 (1.0 g, 1.4 mmol) and benzaldehyde (0.2 g, 1.9 mmol) were dissolved in ethanol (50 mL). After the solution was heated and refluxed for 30 min, a few drops of tetrabutylammonium hydroxide (TBAOH, 2 M solution in water) were added. Then the mixture was refluxed overnight. A yellowish solid was obtained after filtration and washing using water and ethanol. After recrystallization from ethanol, a yellowish powder was obtained (1.0 g, yield 89%). mp > 200 °C. FT-IR: 3291 (NH), 2919, 2850, 1655 (aromatic amide), 1635 (alkyl amide), 1599, and 1527 cm⁻¹. Elemental analysis (%): calculated for C₄₉H₇₅N₅O₄: C, 73.74; H, 9.47; N, 8.77. Found: C, 74.00; H, 9.30; N, 8.70. ¹H NMR (500 MHz, TMS, CDCl₃): 9.14 (s, 1 H, NH), 7.87 (d, J = 9.0 Hz, 2 H), 7.73 (d, J = 10.5 Hz, 2 H), 7.61 (d, J = 10.5 Hz, 2 H), 7.48–7.42 (m, 4 H), 7.18 (d, J = 9.0 Hz, 1 H, NH), 6.92 (t, J = 7.0 Hz, 1 H, NH), 5.87 (t, J = 7.0 Hz, 1 H, NH), 4.43 (q, J = 9.0 Hz, 1 H, C–H), 3.33–3.12 (m, 4 H), 2.50–2.26 (m, 6 H), 2.12–1.90 (m, 4 H), 1.54–1.45 (m, 4 H), 1.22 (m, 36 H), 0.87 (t, J = 8.0 Hz, 6 H). ¹³C NMR (125 MHz, TMS, CDCl₃): 173.3, 172.8, 171.7, 171.6, 140.9, 139.6, 133.8, 130.4, 129.2, 128.9, 126.5, 119.7, 118.0, 111.1, 52.9, 39.9, 39.8, 36.2, 35.0, 32.7, 31.9, 29.6, 29.5, 29.3, 28.8, 27.0, 22.7, 22.0, 14.1.

RESULTS AND DISCUSSION

Gelation Behavior. The gelation ability of 1 in organic solvents was evaluated via a standard heating-and-cooling method.⁸ The results are shown in Table 1. Transparent gels could easily be formed in CHCl₃ and in several aromatic solvents such as benzene, o-dichlorobenzene, and so on. However, compound 1 is soluble in tetrahydrofuran (THF) and DMSO at room temperature without heating. If a quarter volume of water with respect to the volume of DMSO was

Table 1. Gelation Ability of 1 in Various Organic Solvents^a

solvent	status (T _{gel} , °C) ^b	CGC (g/mL %) ^c	solvent	status (T _{gel} , °C)	CGC (w/v %)
cyclohexane	I		acetone	I	
n-hexane	I		ethyl acetate	I	
petroleum ether	I		ethanol	P	
benzene	G (62)	0.08	methanol	G (44)	0.4
toluene	G (65)	0.1	n-octanol	S	
o-dichlorobenzene	G (74)	0.05	xylene	G (84)	0.1
THF	S		DMF	S	
chloroform	G (25)	0.8	DMSO	S	
dichloromethane	G (30)	0.4	DMSO/H ₂ O (4/1 v/v)	G (83)	0.07

^aG, gel; S, soluble; I, insoluble; P, precipitate. ^bT_{gel} is the phase-transition temperature from gel to sol at a concentration of 0.8 g/mL % for chloroform and 0.4 g/mL % for other solvents. ^cCGC is the critical gelation concentration.

added to the DMSO solutions of **1**, then translucent gel phases were obtained (Figure S1). Moreover, the sol–gel transition becomes reversible during the repeated heating–cooling method. However, only the precipitate appeared in the mixture of THF and water. Table 1 also shows the T_{gel} and CGC values. On the basis of the results, the gels of **1** in aromatic solvents and DMSO/H₂O had a higher T_{gel} and a lower CGC relative to those in CH₂Cl₂, CHCl₃, and methanol. In this article, we studied the two-component gels of **1** and **2** in the mixture of DMSO and H₂O. The volume ratio of DMSO and H₂O was 4:1.

Self-Assembly Properties of Gelators in Gel Phases.

The SEM image of gel **1** in DMSO/H₂O was obtained to observe the morphology of the self-assembly of **1** in the gel. As shown in the inset of Figure S2a, numerous intertwined thin fibers with a high aspect ratio (diameter of 50 nm–200 nm, length of several micrometers) were observed. Low-magnification SEM images indicate that these thin fibers extend and assemble to form large junctions (diameter of 200–500 nm) and a fibrous network. Images from the light microscope also indicate the same morphology (Figure S3a). Such micro-morphology seems to be a Cayley tree structure.⁹ The process for network formation can be regarded as initial nucleation–growth–branching–growth–branching.¹⁰

The temperature-dependent UV–vis absorption spectra of compound **1** in DMSO/H₂O were obtained to monitor the interaction between the chromophores during gel formation. As shown in Figure 1a, the absorption band of **1** is located at 340 nm in the solution (100 °C). The band started to blue-shift with decreasing absorption intensity when the temperature was decreased and reached 315 nm at 20 °C. Thus, strong exciton coupling (or a π – π interaction) and the formation of face-to-face packing (an H aggregate) between aromatic moieties occurred.¹¹ In addition, we found that the DMSO solution of **1** emitted weak fluorescence; that is, Φ_F was 0.02. However, upon irradiation of light at a wavelength of 365 nm, the fluorescence of **1** in DMSO/H₂O gradually increased during gelation. Therefore, we checked the change in the fluorescence of **1** in DMSO/H₂O during gel formation. As shown in Figure 1b, the solution of **1** (100 °C) had weak bluish-violet emission ($\lambda_{\text{em}} = 440$ nm), and the emission band gradually red shifted with a continuous enhancement in emission intensity as the temperature was decreased. As a result, the maximum emission for the DMSO/H₂O gel of **1** appeared at 453 nm, and the emission intensity increased by 2.5-fold. The H aggregation generally quenches the fluorescence of the chromophore because the parallel alignment of the chromophores tends to improve the internal conversion from a higher electronic state to a lower one.¹² Therefore, the aggregation-induced enhanced emission in gel **1** may be triggered by the restricted molecular motion during gelation.¹³

In the FT-IR spectrum of the DMSO/H₂O gel of **1**, the antisymmetric and symmetric stretching vibrational bands of CH₂ appeared at 2919 and 2850 cm⁻¹ (Figure S4), respectively, which indicates that the alkyl chains adopted an all-trans extended conformation.¹⁴ This result indicates that the van der Waals interaction among the alkyl chains plays an important role in the self-assembly of **1**. Moreover, the DMSO/H₂O xerogel of **1** showed several bands at 3291 (NH), 1655 (aromatic carbonyl group), and 1634 (alkyl carbonyl group) cm⁻¹, which suggests that all of the amide groups are linked with hydrogen bonds.¹⁵

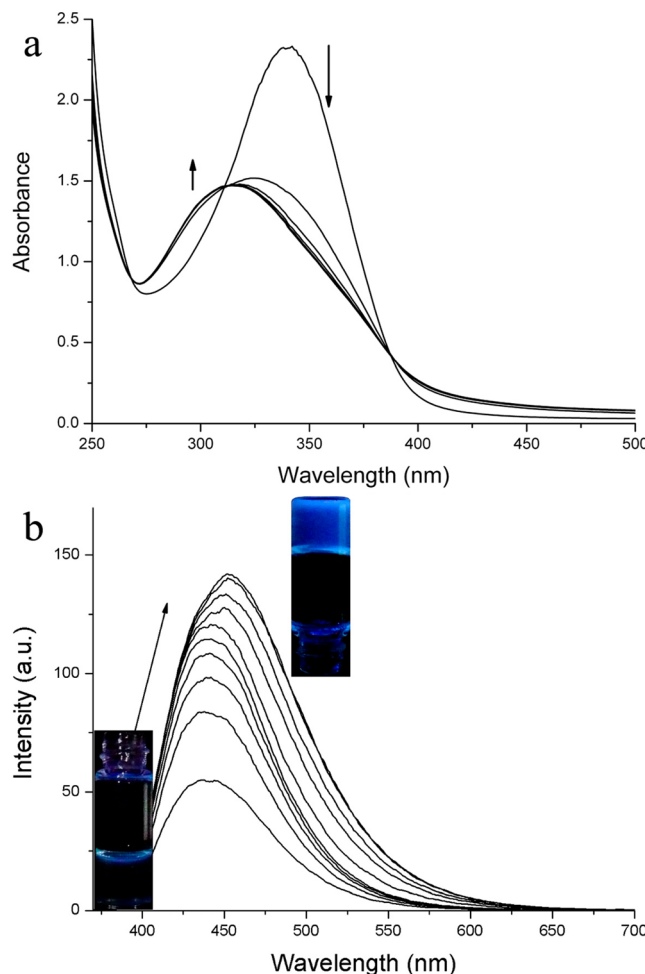


Figure 1. Temperature-dependent (a) UV–vis absorption and (b) fluorescent spectra of **1** in DMSO/H₂O (1.25 mM) from 100 to 20 °C. The interval time is 1 min ($\lambda_{\text{ex}} = 360$ nm).

The ¹H NMR spectra of **1** in *d*₆-DMSO/D₂O gels with different concentrations were obtained to confirm the effect of hydrogen bonds on the gelation of **1**. However, the spectra contained similar weak signals (Figure S5a), which suggests that the gelator molecules aggregate. This aggregation resulted in a reduction of flow even at low concentrations.¹⁶ Therefore, confirming the existence of hydrogen bonding becomes difficult in DMSO/H₂O. However, the gel formed in CDCl₃ had well-resolvable peaks. The UV–vis absorption and IR spectra of the CDCl₃ gel of **1** exhibited similar behavior to those of DMSO/H₂O. The CDCl₃ gel of **1** also showed a 3D nanofibrous structure (Figures S4 and S6), which implies that the intermolecular interactions in CDCl₃ and DMSO/H₂O gels were similar. Therefore, the NMR spectra of the CDCl₃ gel could be used to study the hydrogen bonds.

When the concentration of **1** in CDCl₃ was low (3.7×10^{-3} M), the signals of the four N–H protons appeared at 9.13, 7.08, 6.81, and 5.75 ppm (Figure S5b). These signals were downshifted to 9.19, 7.16, 6.89, and 5.84 ppm, respectively, at a high concentration (2.5×10^{-2} M). The results suggest that all four amide moieties participate in the intermolecular hydrogen bonds rather than in the intramolecular ones.¹⁷ Meanwhile, the signals of amide groups in the ¹H NMR spectra are quite sensitive to temperature. As shown in Figure 2, when the CDCl₃ gel of **1** was heated from 25 to 80 °C the signals

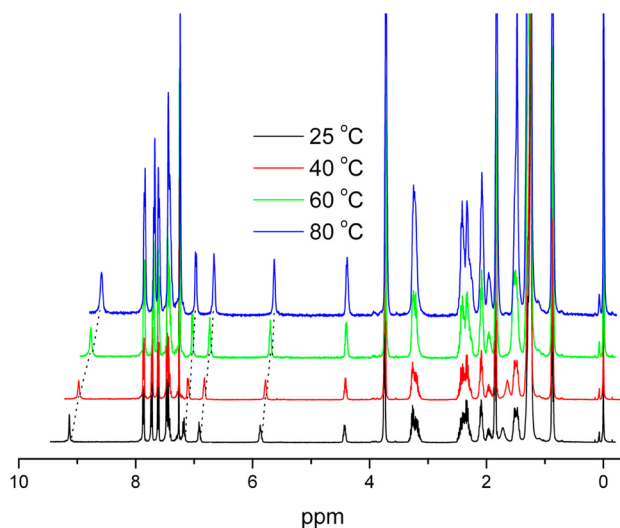


Figure 2. Temperature-dependent ^1H NMR spectra of the CDCl_3 gel of **1** ($2.5 \times 10^{-3} \text{ M}$).

became stronger, which indicates that the signals in the CDCl_3 gel belong to the aggregate. Moreover, the NH peaks were upshifted when the sample was heated, which implies the existence of intermolecular hydrogen bonds between amide units in the gel phase. The intermolecular hydrogen bonds, van der Waals forces, and $\pi-\pi$ stacking interactions promote the aggregation of **1** along a 1D direction to form nanofibrils. These nanofibrils are further entangled into nanofiber-based networks to induce the formation of a gel phase. The FT-IR and NMR spectra results revealed that the hydrogen bonds between N–H and C=O units are intermolecular. Moreover, the UV–vis spectra also indicated that the chromophores of the gelator molecule prefer to self-assemble in a face-to-face mode. The packing model of molecule **1** in a 1D direction in the gel phase is shown in Figure 3a, in which four hydrogen bonds linked the gelator molecules together along the direction of fiber growth. Meanwhile, the theory-stimulated calculation also supported the proposed molecular packing of **1** in the gel phase. The geometric optimization of the gelator molecule was estimated in the AM1 force field, and several optimized molecules were used to simulate the packing model by the energy-minimized optimization in MMFF94.¹⁸ As a result, a stable structure with face-to-face packing could be obtained, as shown in Figure 3b. In this packing model, the distance between two planes of adjacent aromatic moieties is 3.7 Å, which means that the exciton coupling is strong. This result is in agreement with those from the UV–vis absorption spectra. Four amide groups in one molecule can form eight hydrogen bonds with adjacent two molecules. Small-angle X-ray diffraction patterns for DMSO/H₂O of **1** were obtained to demonstrate further the molecular aggregation in long period and to verify the calculation results. Unfortunately, no visible diffraction peaks were observed. Thus, determining the packing mechanism of 1D unimolecular fibers to form a thick fibrillar bundle or determining if the packing is long-range disordered (Figure S7) is difficult. In the wide-angle region, a wide diffraction peak with a maximum at 23.3° corresponding to 3.8 Å was observed. This peak may be used to derive the $\pi-\pi$ packing between aromatic units of **1**, which is close to the calculation value. This result further confirms the face-to-face packing model obtained by the theory-stimulated calculation.

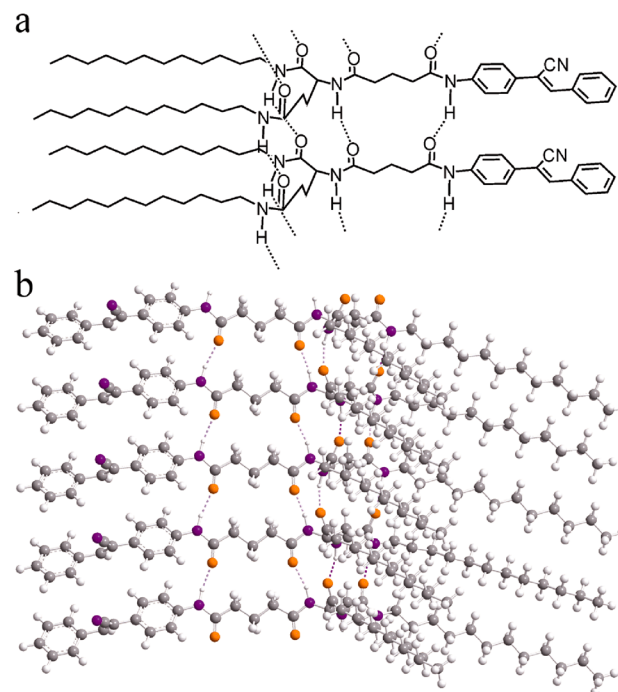


Figure 3. (a) Representation of the self-assembled model with face-to-face packing. (b) Side view of the aggregate of five molecules obtained by energy optimization at the molecular mechanics force field 94 (MMFF94) level of theory.

Energy Transfer and Amplification of Emission Enhancement in a Two-Component Gel Phase. As shown in the section above, gelator **1** can form a gel in DMSO/H₂O with enhanced emission. However, the gel of **1** displayed a low emission intensity because of its inherent low Φ_f and the formation of H aggregates between fluorophores. A highly efficient energy-transfer two-component gel consisting of an acceptor with a large Φ_F and a similar molecular structure to that of **1** must be constructed to obtain a gel with amplifying emission enhancement. **2** is an excellent candidate for the acceptor because it has a similar molecular structure to that of **1** and exhibits strong fluorescence ($\Phi_F = 0.15$ in DMSO). In addition, the emission spectrum of **1** in the gel and the absorption spectrum of **2** in the sol state showed significant spectral overlap (Figure S8, $J(\lambda) = 2.2 \times 10^{13} \text{ M}^{-1} \text{ cm}^{-1} \text{ nm}^4$). Thus, **1** and **2** could cooperatively aggregate to induce co-self-assembly and to obtain a highly efficient excitation energy transfer in a two-component gel.¹⁹

Figure 4a shows the emission spectra of the two-component gels based on **1** and **2** in different molar ratios. Doping gel **1** with **2** as energy traps induced a decrease in the emission (453 nm) of the former. When these energy acceptors were added to form a two-component gel with 1.6 mol % **2**, the emission from **1** was completely quenched, and a new emission band appeared at about 490 nm from **2**. This result indicates that **2** did not form a dimer or an oligomer because the diluted solution of **2** alone at the same concentration ($2.0 \times 10^{-5} \text{ M}$) in DMSO/H₂O also shows an emission band with a maximum of 490 nm (Figure 4b). Moreover, the emission intensity at 490 nm is 5 times greater than that of the solution of **2**. In addition, if the emission wavelength is 550 nm where **1** has a weak emission intensity, the excitation spectrum of the two-component gel has an overlapping excitation band of **1** in the gel state and that of monomeric **2** (Figure S9). The fluorescence lifetime decay

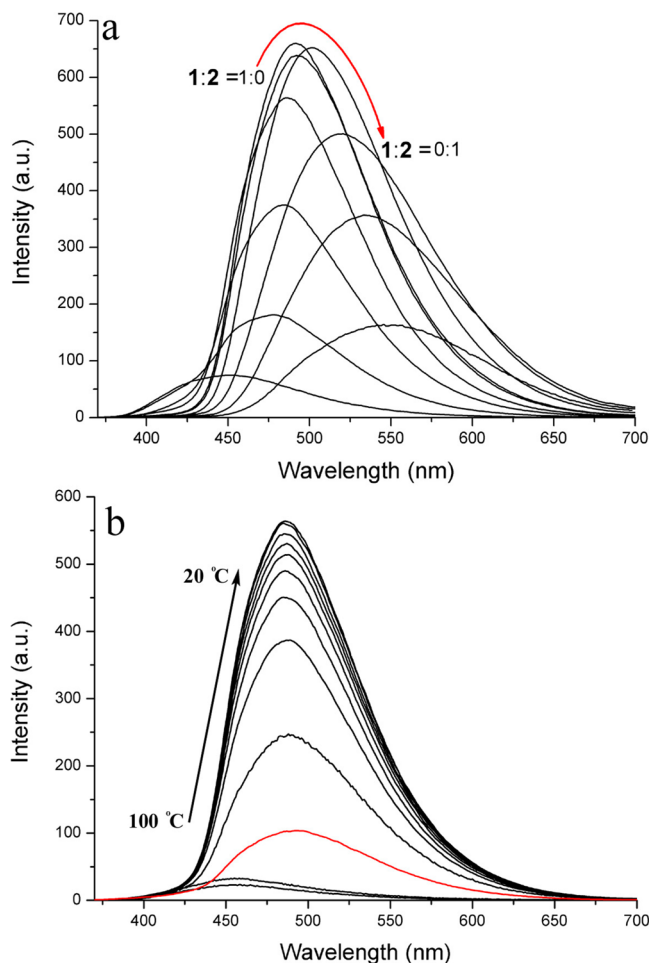


Figure 4. (a) Fluorescence spectra of the mixed gels of **1** and **2** with different molar ratios (0, 0.4, 0.8, 1.6, 3.2, 7.7, 14, 19, 50, and 100 mol % of **2**) in DMSO/H₂O. The concentration of **1** was maintained at 1.25 mM. (b) Fluorescence spectral changes of the mixture of **1** and **2** (1.6 mol % of **2**, 2.0×10^{-5} M) during gelation from 100 to 20 °C. The red line is the emission spectrum of **2** (2.0×10^{-5} M) in DMSO/H₂O ($\lambda_{\text{ex}} = 360$ nm).

profiles ($\lambda_{\text{ex}} = 360$ nm) were monitored at the maximum emission of **2** (490 nm) in the absence and presence of **1** (Figure S10) to verify further the energy transfer from **1** to **2**. The lifetime of **2** in DMSO/H₂O (2.0×10^{-5} M) was 0.87 ns, which was prolonged to 1.76 ns in the presence of donor **1**.

These observations revealed compelling evidence for highly efficient energy transfer from **1** to **2**.^{19,20}

The emission of the mixed solution of **1** and **2** (1.6 mol % of **2**) at 100 °C was weak at an excitation wavelength of 360 nm. Moreover, the fluorescence intensity of the gel increased 23-fold (Figure 4b), which indicates that the amplifying emission was enhanced (Figure S11). Therefore, the use of an acceptor with a large Φ_F contributed to the success of obtaining a strongly emitting gel. Figure 4a also shows that the peak at 490 nm from monomeric **2** started to red shift when the concentration of **2** was more than 7.7 mol %. This result indicates that **2** started to form a dimer or an oligomer by itself.²¹ The absorption spectra also verified this phenomenon (Figure S12). As a result, tunable emissions of more than 100 nm in two-component gels can be operated by simply adjusting the amount of the acceptor (Figures S13 and S14).²²

Light microscopy, SEM, and fluorescence microscopy images were performed to obtain further insight into the self-assembly of gelators in a two-component gel. The gel became more transparent with increasing amounts of **2**, and 50 mol % **2** resulted in the formation of a transparent gel (Figure S14). This result suggests that adding **2** may change the morphology of the gel. When a small amount of **2**, such as 0.8 mol % (Figures S2b and S3b), was added to the gel of **1**, the gel maintained its morphology of having a large radiating fibrous network. However, when the amount of **2** was gradually increased, some thin fibers appeared in the gel phase, and these fibers became thinner when **2** was added to **1** (Figures S2 and S3). When the molar ratio of **1** to **2** was 1:1, the two-component gel was composed of thin fibers that are similar to those of the gel of **2**. This composition may be the reason why this two-component gel is clear and transparent. This observation clearly suggests that the addition of **2** strongly influences the morphology of the gel matrix.

If **2** was uniformly embedded in the gel scaffold of **1** remains to be clarified. Thus, fluorescence microscopy images were obtained. As shown in Figure 5, the fibers of the gel in the absence of **2** resulted in a blue-violet emission. The fiber of the gel with 0.8 mol % **2** resulted in a uniform bright-blue emission (Figure S15a), which suggests that the acceptor was uniformly dispersed in the donor fiber.²³ The junctions of the radiating fibrous networks resulted in a brighter emission. When the amount of **2** was increased to 14 mol %, the coassembled fibers had a uniform greenish blue emission (Figure S15b). Some bright dots were also observed, which may be due to small

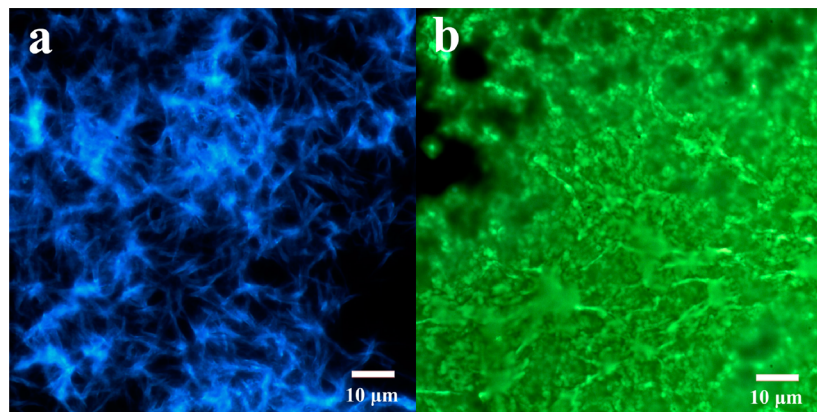


Figure 5. Fluorescence microscopy images of DMSO/H₂O xerogels of (a) **1** and (b) **2**. The excitation wavelengths for a and b are 330–385 nm.

junctions because some small radiating networks are present (Figure S3d). These observations strongly support the occurrence of homogeneous coassembly in the gel with a low concentration of **2**, thereby promoting highly efficient energy transfer between the excited donors and the acceptor in the ground state.

Proton Response of Two-Component Gels. **2** may function as a sensory material for detecting H^+ because the benzimidazole moiety in compound **2** can be protonated to form a cation.²⁴ As shown in Figure S16a, the emission of **2** in DMSO has a bathochromic shift upon the addition of TFA upon excitation at 400 nm. For example, the emission band at 498 nm red-shifted to 560 nm after the addition of 10 equiv of TFA. Moreover, the plot of the fluorescence intensity at 500 nm versus the molar ratio of $[\text{TFA}]/[2]$ showed an inflection at a molar ratio of $[\text{TFA}]/[2] = 1$, which indicates the formation of a 1:1 complex (2H^+) between H^+ and **2** in DMSO.²⁵ As shown in Figure S13b, the Hill plot was obtained to evaluate the binding constant ($\log K_{\text{ass}}$) and binding number (n) of **2** for the proton.²⁶ $\log K_{\text{ass}}$ was 4.25, which indicates that **2** has a strong binding affinity for H^+ . n was 0.96, which also shows that **2** binds with H^+ in a ratio of 1:1. However, the emission intensity of the DMSO/ H_2O gel of **1** slightly decreased upon the addition of TFA (Figure S17) because of the absence of proton binding site. This decrease may be due to the change in the microenvironment around the gel fibers. This result suggests that the gel of **1** can function as an excellent scaffold for studying the proton response of **2** inserted into the gel fibers of **1**.

When TFA was added to the hot DMSO/ H_2O solution of the mixture of **1** and **2** in which the molar content of **2** was less than 50 mol %, a weak yellow fluorescence was observed upon irradiation of light at 365 nm. The fluorescence spectrum of the hot solution with 7.7 mol % **2** can be regarded as the overlap of two peaks at 440 and 550 nm (Figure 6a). These peaks can be ascribed to the emission bands of **1** and 2H^+ , respectively. The hot solution with 7.7 mol % **2** had a single emission band with a maximum at 550 nm when **2** alone was excited at 400 nm (Figure 6b). These observations suggest that the benzimidazole moiety of **2** was bound to the proton to form a corresponding cation (2H^+) in a hot solution in the presence of TFA. When the mixture was gradually cooled to room temperature to form the two-component gel, the fluorescence of the system became increasingly stronger and the gel exhibited blue-green emission (Figure 6c). In the emission spectra of the two-component gel with TFA ($\lambda_{\text{ex}} = 360$ nm), the overlapping emission band with double peaks was replaced by the emission band with a maximum at 502 nm. At an excitation wavelength of 400 nm, this gel also exhibited a blue-shifted emission band with a maximum at 508 nm. A slight red shift of 9 nm (from 493 to 502 nm) and an obvious decrease in emission intensity were observed after the addition of TFA when excited at 360 nm. Moreover, other mixtures with less than 50 mol % **2** have similar emission behaviors (Figure S18 and S19). The emission behaviors of mixtures with low concentrations of **2** before and after the addition of TFA are shown in Figure S20. In the absence of TFA, the system emitted strong blue-green fluorescence from **2** when the hot solution with weak emission was turned into the gel phase because of the highly efficient energy transfer from donor **1** to acceptor **2**. As a result, an amplifying emission enhancement occurred in the two-component gel. In the presence of TFA, monomeric **1** and 2H^+ in the hot solution had weak emission bands. When the

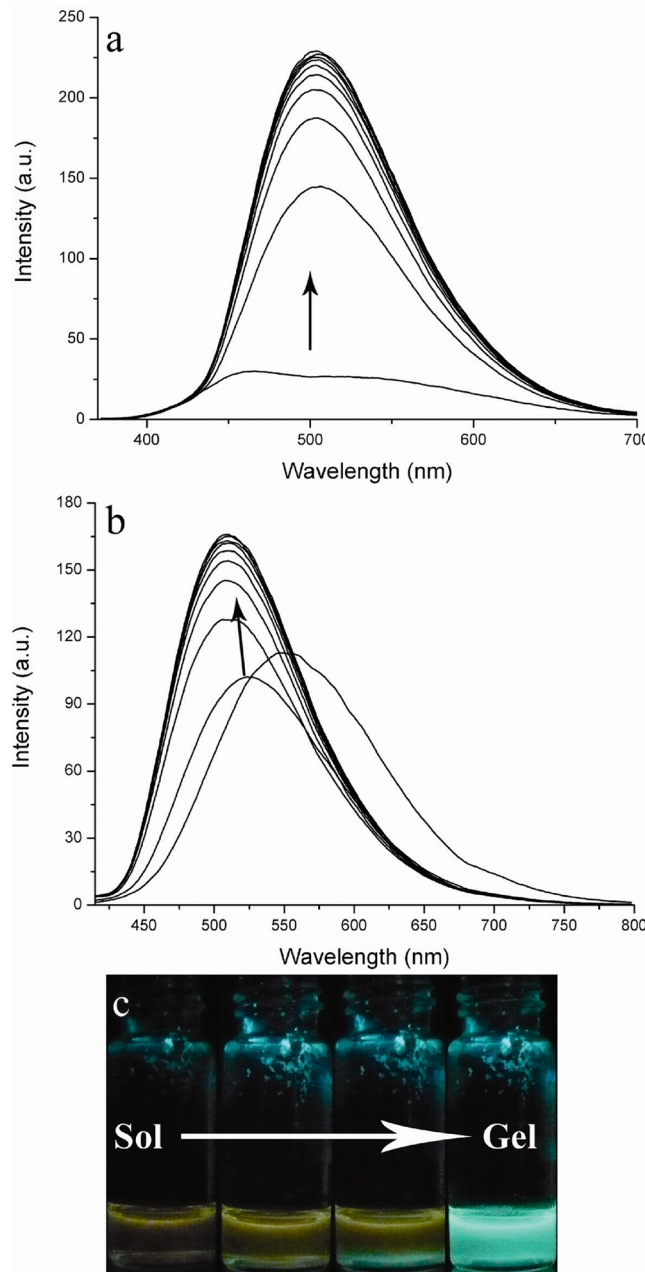


Figure 6. Change in the fluorescence spectra of the mixture with 7.7 mol % **2** and TFA during gelation for excitation at (a) 360 and (b) 400 nm. (c) Optical images of the gelation process of the mixture with TFA and 7.7 mol % **2** upon irradiation of light at 365 nm. Arrows show the gelation process from sol to gel.

temperature was gradually decreased, molecule **1** began to aggregate. Meanwhile, some 2H^+ molecules can adsorb on the top of these aggregates because of the formation of hydrogen bonds between **1** and 2H^+ . However, a large steric hindrance and a repulsive interaction between neutral molecules and the cation (2H^+) during coassembly might occur, which prevents **2** from strongly binding with H^+ . Therefore, the interaction between **2** and H^+ was significantly weakened during gelation, which induced the blue shift in the emission band. Thus, we can obtain distinctive responses to external stimuli by introducing an active unit in the inert gel scaffold.

The wet two-component gels had a favorable response to the proton. We then studied the behavior of the xerogel film in

response to the proton. The result showed that xerogel films with intense emission had weak, red-shifted fluorescence after they were soaked in hydrochloric acid. This result indicated that **2** in the xerogel films could interact with the proton to form complex **2H⁺**. These xerogel films also showed a good response to vapors of volatile acids, such as TFA, hydrochloric acid (HCl), acetic acid, and so on. Figure 7 shows an example of a

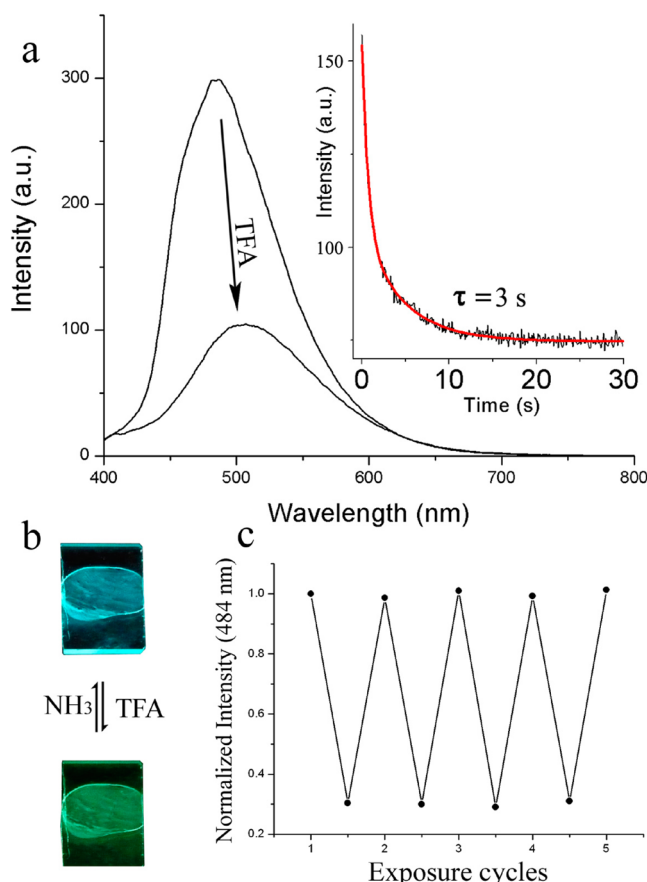


Figure 7. (a) Emission spectra of a DMSO/H₂O xerogel film with 7.7 mol % **2** after exposure to TFA- and NH₃-saturated vapor. The inset shows the time course of emission quenching at 490 nm. $\lambda_{\text{ex}} = 360$ nm. (b) Photographs of films after exposure to TFA and NH₃ vapor upon irradiation with 365 nm light. (c) Fluorescence cycles generated by exposing the xerogel film to the saturated vapor of TFA and NH₃. The fluorescence intensities at 484 nm were normalized to the initial value before exposure to the saturated vapor of TFA.

xerogel film with 7.7 mol % **2**. The fluorescent color of the xerogel film could rapidly change from light blue to blue-green (Figure 7b) after exposure to TFA vapor. Moreover, the fluorescence of the film became weak and the emission band had a bathochromic shift from 486 to 507 nm. A shift of 23 nm suggests that acceptor **2** in coassembly also binds to the gaseous acid. The inset in Figure 7a shows the fluorescence change in the film after exposure to TFA vapor. The average response time (τ) for the quenching process (defined as the decay lifetime) can be deduced by fitting the intensity decay to double-exponential kinetics. The xerogel film with 7.7 mol % **2** had a short response time of about 3 s. The short response time was mainly caused by the 3D, continuous, porous structure formed by entangled nanofibers. These nanofibers provide pathways for the TFA molecules to diffuse throughout the film matrix and readily interact with **2**.²⁷ The fluorescence of films

exposed to the vapor of TFA could be rapidly recovered by exposing the film to NH₃ vapor. The average responsive time of this film was 1.3 s (Figure S21). This process could be reversibly repeated many times, and similar efficient responses were obtained with repeated use. This result implies the stability of this xerogel film. After the xerogel films were exposed to other acids such HCl and acetic acid, the films had a similar change in the spectra to that in the TFA vapor (Figure S22). However, the exposure to acetic acid resulted in a smaller shift because acetic acid is a weak acid. Moreover, the fluorescence changes in mixed gel films were measured after exposure to other solvents. The emission intensities of the films decreased by different degrees, and the emission band was not shifted. The intensities reverted to their original values when the exposure of the films to solvent vapors was stopped. As described above, the emission of the films was red-shifted after exposure to acid vapors, and their emission could be quenched. However, the fluorescence was not recovered when the exposure of the films to the acid vapors was stopped. Thus, our film can selectively recognize volatile acid.²⁸

CONCLUSIONS

Glutamide gelator **1** was synthesized, and a weak emission enhancement (2.5-fold increase) was observed during its gelation. Energy acceptor **2** with a high Φ_F was used to construct two-component gels with **1**. Two-component gels always had stronger emission, and an amplifying emission enhancement was observed compared to that of the gel of **1**. The two-component gels showed a favorable response to protons. With low concentrations of the acceptor, the hot solution emitted yellow fluorescence upon the addition of the proton. This emission was blue-shifted and enhanced after gel formation because the binding of **2** with the proton is weakened during coassembly. Moreover, the casting films also had an excellent response to volatile acids such as hydrochloric acid, TFA, and so on. The emission of these films could be reversibly recovered by exposure to NH₃. This work suggests that two-component gels are promising candidates as functional materials for several typical applications.

ASSOCIATED CONTENT

Supporting Information

IR and NMR spectra; photographic, microscopy, and SEM images. Absorption, excitation, and emission spectra of the two-component gel and gels of **1** and **2** before and after proton addition. Proton titration experiment of the fluorescence of **2**. Schematic representation of the two-component gel. Recovery curve of film fluorescence. This material is available free of charge via the Internet at <http://pubs.acs.org>.

AUTHOR INFORMATION

Corresponding Author

*E-mail: xuepengchong@jlu.edu.cn; luran@mail.jlu.edu.cn.

Notes

The authors declare no competing financial interest.

ACKNOWLEDGMENTS

This article was written through the contributions of all authors, and all authors have given approval to the final version of the article. This work was financially supported by the National Natural Science Foundation of China (21103067, 91127005, 20874034, and 51073068), the 973 Program (2009CB939701),

the NSFC-JSPS Scientific Cooperation Program (21011140069), the Open Project of the State Key Laboratory of Supramolecular Structure and Materials (SKLSSM201203), and the Open Project Program of Key Laboratory of Photochemical Conversion and Optoelectronic Materials, Technical Institute of Physics and Chemistry, Chinese Academy of Sciences.

■ REFERENCES

- (1) (a) Brunsved, L.; Folmer, B. J. B.; Meijer, E. W.; Sijbesma, R. P. Supramolecular polymers. *Chem. Rev.* **2001**, *101*, 4071. (b) Elemans, J. A. A. W.; Rowan, A. E.; Nolte, R. J. M. Mastering molecular matter. Supramolecular architectures by hierarchical self-assembly. *J. Mater. Chem.* **2003**, *13*, 2661. (c) Pollino, J. M.; Weck, M. Non-covalent side-chain polymers: design principles, functionalization strategies, and perspectives. *Chem. Soc. Rev.* **2005**, *34*, 193. (d) Cravotto, G.; Cintas, P. Molecular self-assembly and patterning induced by sound waves. The case of gelation. *Chem. Soc. Rev.* **2009**, *38*, 2684.
- (2) (a) Terech, P.; Weiss, R. G. Low molecular mass gelators of organic liquids and the properties of their gels. *Chem. Rev.* **1997**, *97*, 3133. (b) van Esch, J. H.; Feringa, B. L. New functional materials based on self-assembling organogels: from serendipity towards design. *Angew. Chem., Int. Ed.* **2000**, *39*, 2263. (c) Estroff, L. A.; Hamilton, A. D. Water gelation by small organic molecules. *Chem. Rev.* **2004**, *104*, 1201. (d) Hirst, A. R.; Smith, D. K. Two-component gel-phase materials-highly tunable self-assembling systems. *Chem.—Eur. J.* **2005**, *11*, 5496. (e) Brizard, A.; Oda, R.; Huc, I. Chirality effects in self-assembled fibrillar networks. *Top. Curr. Chem.* **2005**, *256*, 167. (f) Ajayaghosh, A.; Praveen, V. K. π -Organogels of self-assembled p-phenylenevinylenes: soft materials with distinct size, shape, and functions. *Acc. Chem. Res.* **2007**, *40*, 644. (g) Piepenbrock, M. M.; Lloyd, G. O.; Clarke, N.; Steed, J. W. Metal- and anion-binding supramolecular gels. *Chem. Rev.* **2010**, *110*, 1960.
- (3) (a) Yang, Z.; Liang, G.; Xu, B. Enzymatic hydrogelation of small molecules. *Acc. Chem. Res.* **2008**, *41*, 315. (b) Zhang, Y. M.; Lin, Q.; Wei, T. B.; Qin, X. P.; Li, Y. A novel smart organogel which could allow a two channel anion response by proton controlled reversible sol-gel transition and color changes. *Chem. Commun.* **2009**, 6074. (c) Wu, X.; Ji, S.; Li, Y.; Li, B.; Zhu, X.; Hanabusa, K.; Yang, Y. Helical transfer through nonlocal interactions. *J. Am. Chem. Soc.* **2009**, *131*, 5986. (d) Wicklein, A.; Ghosh, S.; Sommer, M.; Würthner, F.; Thelakkat, M. Self-assembly of semiconductor organogelator nanowires for photoinduced charge separation. *ACS Nano* **2009**, *3*, 1107. (e) Xue, P. C.; Lu, R.; Huang, Y.; Jin, M.; Tan, C. H.; Bao, C. H.; Wang, Z. M.; Zhao, Y. Y. Novel pearl-necklace porous CdS nanofiber templated by organogel. *Langmuir* **2004**, *20*, 6470. (f) Haines, S. R.; Harrison, R. G. Novel resorcinarene-based pH-triggered gelator. *Chem. Commun.* **2002**, 2846. (g) Vintiloiu, A.; Leroux, J. C. Organogels and their use in drug delivery—a review. *J. Controlled Release* **2008**, *125*, 179. (h) Lozano, V.; Hernández, R.; Ardá, A.; Jiménez-Barbero, J.; Mijangos, C.; Pérez-Pérez, M. An asparagine/tryptophan organogel showing a selective response towards fluoride anions. *J. Mater. Chem.* **2011**, *21*, 8862. (i) Ajayaghosh, A.; Praveen, V. K.; Vijayakumar, C. Organogels as scaffolds for excitation energy transfer and light harvesting. *Chem. Soc. Rev.* **2008**, *37*, 109. (j) Edelsztein, V. C.; Burton, G.; Chenna, P. H. D. Self-assembly of a silylated steroid-based organogelator and its use as template for the in situ sol-gel polymerization of tetraethyl orthosilicate. *Tetrahedron* **2010**, *66*, 2162.
- (4) (a) Sugiyasu, K.; Kawano, S.; Fujita, N.; Shinkai, S. Self-sorting organogels with p-n heterojunction points. *Chem. Mater.* **2008**, *20*, 2863. (b) Das, R. K.; Banerjee, S.; Raffy, G.; Guerzo, A. D.; Desvergne, J.; Maitra, U. Spectroscopic, microscopic and first rheological investigations in charge-transfer interaction induced organogels. *J. Mater. Chem.* **2010**, *20*, 7227. (c) Adhikari, B.; Nanda, J.; Banerjee, A. Pyrene-containing peptide-based fluorescent organogels: inclusion of graphene into the organogel. *Chem.—Eur. J.* **2011**, *17*, 11488. (d) Prasanthkumar, S.; Gopal, A.; Ajayaghosh, A. Self-assembly of thiylenevinylene molecular wires to semiconducting gels with doped metallic conductivity. *J. Am. Chem. Soc.* **2010**, *132*, 13206.
- (5) (a) Yang, X. C.; Lu, R.; Xue, P. C.; Li, B.; Xu, D. F.; Xu, T. H.; Zhao, Y. Y. Carbazole-based organogel as a scaffold to construct energy transfer arrays with controllable fluorescence emission. *Langmuir* **2008**, *24*, 13730. (b) Vijayakumar, C.; Praveen, V. K.; Ajayaghosh, A. RGB emission through controlled donor self-Assembly and modulation of excitation energy transfer: a novel strategy to white-light-emitting organogels. *Adv. Mater.* **2009**, *21*, 2059. (c) Vijayakumar, C.; Praveen, V. K.; Kartha, K. K.; Ajayaghosh, A. Excitation energy migration in oligo(p-phenylenevinylene) based organogels: structure-property relationship and FRET efficiency. *Phys. Chem. Chem. Phys.* **2011**, *13*, 4942. (d) Abbel, R.; van der Weegen, R.; Pisula, W.; Surin, M.; Leclère, P.; Lazzaroni, R.; Meijer, E. W.; Schenning, A. P. H. J. Multicolour self-assembled fluorene co-oligomers: from molecules to the solid state via white-light-emitting organogels. *Chem.—Eur. J.* **2009**, *15*, 9737.
- (6) (a) Totsatitpaisan, P.; Nunes, S. P.; Tashiro, K.; Chirachanchai, S. Investigation of the role of benzimidazole-based model compounds on thermal stability and anhydrous proton conductivity of sulfonated poly(ether ether ketone). *Solid State Ionics* **2009**, *180*, 738. (b) Shen, L.; Zhao, P.; Zhu, W. A ratiometric hydrophilic fluorescent copolymer sensor based on benzimidazole chromophore for microbioreactors. *Dyes Pigments* **2011**, *89*, 236. (c) Matthews, C. J.; Broughton, V.; Bernardinelli, G.; Melich, X.; Brand, G.; Willisc, A. C.; Williams, A. F. Molecular bricklaying: the protonated benzimidazole moiety as a synthon for crystal engineering. *New J. Chem.* **2003**, *27*, 354.
- (7) Xue, P. C.; Lu, R.; Zhao, L.; Xu, D. F.; Zhang, X. F.; Li, K. C.; Song, Z. G.; Yang, X. C.; Takafuji, M.; Ihara, H. Hybrid self-assembly of a π gelator and fullerene derivative with photoinduced electron transfer for photocurrent generation. *Langmuir* **2010**, *26*, 6669.
- (8) Zhang, X. F.; Lu, R.; Jia, J. H.; Liu, X. L.; Xue, P. C.; Xu, D. F.; Zhou, H. P. Organogel based on β -diketone-boron difluoride without alkyl chain and H-bonding unit directed by optimally balanced π - π interaction. *Chem. Commun.* **2010**, *46*, 8419.
- (9) Shi, J. H.; Liu, X. Y.; Li, J. L.; Strom, C. S.; Xu, H. Y. Spherulitic networks: from structure to rheological property. *J. Phys. Chem. B* **2009**, *113*, 4549.
- (10) Tang, S.; Liu, X. Y.; Strom, C. S. Producing supramolecular functional materials based on fiber network reconstruction. *Adv. Funct. Mater.* **2009**, *19*, 2252.
- (11) (a) Kash, M.; Rawls, H. R.; El-Bayoumi, M. A. The exciton model in molecular spectroscopy. *Pure Appl. Chem.* **1965**, *11*, 371. (b) Yagai, S.; Higashi, M.; Karatsu, T.; Kitamura, A. Dye-assisted structural modulation of hydrogen-bonded binary supramolecular polymers. *Chem. Mater.* **2005**, *17*, 4392. (c) Lewis, F. D.; Liu, X.; Wu, Y.; Zuo, X. Stepwise evolution of the structure and electronic properties of DNA. *J. Am. Chem. Soc.* **2003**, *125*, 12729.
- (12) (a) An, B.; Kwon, S.; Jung, S.; Park, S. Y. Enhanced emission and its switching in fluorescent organic nanoparticles. *J. Am. Chem. Soc.* **2002**, *124*, 14410. (b) Xue, P. C.; Lu, R.; Chen, G. J.; Zhang, Y.; Nomoto, H.; Takafuji, M.; Ihara, H. Functional organogel based on a salicylideneaniline derivative with enhanced fluorescence emission and photochromism. *Chem.—Eur. J.* **2007**, *13*, 8231.
- (13) (a) Bao, C. Y.; Lu, R.; Jin, M.; Xue, P. C.; Tan, C. H.; Liu, G. F.; Zhao, Y. Y. L-Tartaric acid assisted binary organogel system: strongly enhanced fluorescence induced by supramolecular assembly. *Org. Biomol. Chem.* **2005**, *3*, 2508. (b) Chen, Y. L.; Lv, Y. X.; Han, Y.; Zhu, B.; Zhang, F.; Bo, Z. S.; Liu, C. Y. Dendritic effect on supramolecular self-assembly: organogels with strong fluorescence emission induced by aggregation. *Langmuir* **2009**, *25*, 8548. (c) Kumar, N. S. S.; Varghese, S.; Narayan, G.; Das, S. Hierarchical self-assembly of donor–acceptor-substituted butadiene amphiphiles into photoresponsive vesicles and gels. *Angew. Chem., Int. Ed.* **2006**, *45*, 6317. (d) Rösch, U.; Yao, S.; Wortmann, R.; Würthner, F. Fluorescent H-aggregates of merocyanine dyes. *Angew. Chem., Int. Ed.* **2006**, *45*, 7026.
- (14) (a) Masuda, M.; Vill, V.; Shimizu, T. Conformational and thermal phase behavior of oligomethylene chains constrained by carbohydrate hydrogen-bond networks. *J. Am. Chem. Soc.* **2000**, *122*,

12327. (b) Rahman, M. M.; Czaun, M.; Takafuji, M.; Ihara, H. Synthesis, self-assembling properties, and atom transfer radical polymerization of an alkylated l-phenylalanine-derived monomeric organogel from silica: a new approach to prepare packing materials for high-performance liquid chromatography. *Chem.—Eur. J.* **2008**, *14*, 1312.
- (15) (a) Amada, N.; Ariga, K.; Naito, M.; Matsubara, K.; Koyama, E. Regulation of β -sheet structures within amyloid-like β -sheet assemblage from tripeptide serivatives. *J. Am. Chem. Soc.* **1998**, *120*, 12192. (b) Suzuki, M.; Setoguchi, C.; Shirai, H.; Hanabusa, K. Organogelation by polymer organogelators with a L-lysine derivative: formation of a three-dimensional network consisting of supramolecular and conventional polymers. *Chem.—Eur. J.* **2007**, *13*, 8193. (c) Liu, J.; He, P.; Yan, J.; Fang, X.; Peng, J.; Liu, K.; Fan, Y. An organometallic super-gelator with multiple-stimulus responsive properties. *Adv. Mater.* **2008**, *20*, 2508. (d) Lozano, V.; Hernández, R.; Mijangos, C.; Pérez-Pérez, M. A novel organogelator incorporating tert-butyl esters of asparagines. *Org. Biomol. Chem.* **2009**, *7*, 364.
- (16) (a) Tata, M.; John, V. T.; Waguespack, Y. Y.; McPherson, G. L. Intercalation in novel organogels with a “stacked” phenol microstructure. *J. Am. Chem. Soc.* **1994**, *116*, 9464. (b) Shapiro, Y. E. Structure and dynamics of hydrogels and organogels: an NMR spectroscopy approach. *Prog. Polym. Sci.* **2011**, *36*, 1184.
- (17) (a) Yang, X.; Zhang, G.; Zhang, D.; Zhu, D. A new ex-TTF-based organogelator: formation of organogels and tuning with fullerene. *Langmuir* **2010**, *26*, 11720. (b) Samai, S.; Dey, J.; Biradha, K. Amino acid based low-molecular-weight tris(bis-amido) organogelators. *Soft Matter* **2011**, *7*, 2121. (c) Hou, X.; Gao, D.; Yan, J.; Ma, Y.; Liu, K.; Fang, Y. Novel dimeric cholesteryl derivatives and their smart thixotropic gels. *Langmuir* **2011**, *27*, 12156.
- (18) (a) Wang, M.; Zheng, Y.; Cook, T. R.; Stang, P. J. Construction of functionalized metallasupramolecular tetragonal prisms via multi-component coordination-driven self-assembly. *Inorg. Chem.* **2011**, *50*, 6107. (b) Dawn, S.; Dewal, M. B.; Sobransingh, D.; Paderes, M. C.; Wibowo, A. C.; Smith, M. D.; Krause, J. A.; Pellechia, P. J.; Shimizu, L. S. Porous crystals from self-assembled phenylethylenylene bis-urea macrocycles facilitate the selective photodimerization of coumarin. *J. Am. Chem. Soc.* **2011**, *133*, 7025.
- (19) (a) Valeur, B. *Molecular Fluorescence: Principles and Applications*; Wiley-VCH: Weinheim, Germany, 2002. (b) Ajayaghosh, A.; Praveen, V. K.; Vijayakumar, C.; George, S. J. Molecular wire encapsulated into π organogels: efficient supramolecular light-harvesting antennae with color-tunable emission. *Angew. Chem., Int. Ed.* **2007**, *46*, 6260.
- (20) (a) Babu, S. S.; Kartha, K. K.; Ajayaghosh, A. Excited state processes in linear π -system-based organogels. *J. Phys. Chem. Lett.* **2010**, *1*, 3413.
- (21) Ajayaghosh, A.; Vijayakumar, C.; Praveen, V. K.; Babu, S. S.; Varghese, R. Self-location of acceptors as “isolated” or “stacked” energy traps in a supramolecular donor self-assembly: a strategy to wavelength tunable FRET emission. *J. Am. Chem. Soc.* **2006**, *128*, 7174.
- (22) Shu, T.; Wu, J.; Lu, M.; Chen, L.; Yi, T.; Li, F.; Huang, C. Tunable red–green–blue fluorescent organogels on the basis of intermolecular energy transfer. *J. Mater. Chem.* **2008**, *18*, 886.
- (23) Guerzo, D.; Olive, A. G. L.; Reichwagen, J.; Hopf, H.; Desvergne, J. P. Energy transfer in self-assembled $[n]$ -acene fibers involving ≥ 100 donors per acceptor. *J. Am. Chem. Soc.* **2005**, *127*, 17984.
- (24) (a) Muñiz, F. M.; Alcázar, V.; Sanz, F.; Simón, L.; de Arriba, Á. L. F.; Raposo, C.; Morán, J. R. A xanthene–benzimidazole receptor with multiple H-bond donors for carboxylic acids. *Eur. J. Org. Chem.* **2010**, 6179. (b) Xue, P. C.; Lu, R.; Jia, J. H.; Takafuji, M.; Ihara, H. A smart gelator as a chemosensor: application to integrated logic gates in solution, gel, and film. *Chem.—Eur. J.* **2012**, *18*, 3549.
- (25) (a) Džolić, Z.; Cametti, M.; Cort, A. D.; Mandolini, L.; Žinić, M. Fluoride-responsive organogelator based on oxalamide-derived anthraquinone. *Chem. Commun.* **2007**, 3535. (b) Kim, D.; Ahn, K. H. Fluorescence “turn-on” sensing of carboxylate anions with oligothiophene-based α -(carboxamido)trifluoroacetophenones. *J. Org. Chem.* **2008**, *73*, 6831. (c) Quinlan, E.; Matthews, S. E.; Gunnlaugsson, T. Colorimetric recognition of anions using preorganized tetraamidourea derived calix[4]arene sensors. *J. Org. Chem.* **2007**, *72*, 7497. (d) Xu, D. F.; Liu, X. L.; Lu, R.; Xue, P. C.; Zhang, X. F.; Zhou, H. P.; Jia, J. H. New dendritic gelator bearing carbazole in each branching unit: selected response to fluoride ion in gel phase. *Org. Biomol. Chem.* **2011**, *9*, 1523.
- (26) Huang, W.; Su, H.; Yao, S.; Lin, H.; Cai, Z.; Lin, H. A simple and neutral receptor acting as a sensitive and switch-on fluorescent chemosensor for H_2PO_4^- . *J. Fluoresc.* **2011**, *21*, 1697.
- (27) (a) Che, Y.; Yang, X.; Zhang, Z.; Zuo, J.; Moore, J. S.; Zang, L. Ambient photodoping of p-type organic nanofibers: highly efficient photoswitching and electrical vapor sensing of amines. *Chem. Commun.* **2010**, *46*, 4127. (b) Che, Y.; Yang, X.; Loser, S.; Zang, L. Expedient vapor probing of organic amines using fluorescent nanofibers fabricated from an n-type organic semiconductor. *Nano Lett.* **2008**, *8*, 2219.
- (28) (a) Wang, H.; He, G.; Chen, X.; Liu, T.; Ding, L.; Fang, Y. Cholesterol modified OPE functionalized film: fabrication, fluorescence behavior and sensing performance. *J. Mater. Chem.* **2012**, *22*, 7529. (b) Cox, R. P.; Higginbotham, H. F.; Graystone, B. A.; Sandanayake, S.; Langford, S. J.; Bell, T. D. M. A new fluorescent H^+ sensor based on core-substituted naphthalene diimide. *Chem. Phys. Lett.* **2012**, *521*, 59. (c) A transparent TMPyP/TiO₂ composite thin film as an HCl sensitive optochemical gas sensor. Cano, M.; Castillero, P.; Roales, J.; Pedrosa, J. M.; Brittle, S.; Richardson, T.; González-Elipe, A. R.; Barranco, A. *Sens. Actuators, B* **2012**, *150*, 764.